



Study of the Contrast Observed on Carbon by Monte Carlo Simulation on wet-STEM Tomography

Rahmat Firman Septiyanto^{1,a} and Isriyanti Affifah²

¹Department of Physics Education, Universitas Sultan Ageng Tirtayasa, Serang, Indonesia

²Department of Chemistry Education, Universitas Sultan Ageng Tirtayasa, Serang, Indonesia

^arahmat_firman99@untirta.ac.id

Abstract. Analyzing the structure of the material in the fields of material science needs a perfect device and methods. Due to its principle in projected images at various tilt angles and calculating the three-dimensional volume reconstruction with a unique algorithm, tomography has become an excellent tool for analyzing the 3D structure. Much research has been studied on applying electron tomography in ESEM (Environmental Scanning Electron Microscopy), which allows observing the wet material (hydrated) in the aquatic environment. In this research, we showed the advisability of wet-Carbon compound tomography by simulating the interaction of electron materials. Monte Carlo simulation was applied in this study to calculate the optimum water layer thickness in the wet material detected.

Keywords: Carbon, Electron Tomography, Simulation of Monte Carlo, STEM.

Introduction

Water is a suitable solvent for both organic and inorganic materials. Some typical materials could contain water in various concentrations or even be dispersed in the water itself [1]. There are several examples of this phenomenon, such as specimens of living cells (which contain a vast water fraction), biopolymer suspensions (its polymer is water-dispersed), and ceramics (dispersed in a liquid in the process to gain a high density) [2-4].

Carbon is involved in biological processes and is contained and or dispersed in water through chemical or physical processes. Electron microscopy is an essential technique in understanding the dispersion in suspension and the material's properties at the nanoscale study [5].

The previous study showed that the liquid suspensions could also be learned by using Environmental Scanning Electron Microscopy (ESEM). The pressure in the sample chamber can reach several tens of Torr with differential pumping. The function of the Peltier phase in ESEM observes a fully hydrated state object possible [6,7]. Changing the pressure of the sample chamber could directly carry out the water condensation and evaporation. The observation of wet material was perfectly shown in ESEM using backscattering electron detectors or secondary electrons [7]; a collection of sensors placed under a liquid droplet has proven to be an efficient observation mode [8].

Tomography plays an essential role in the material characterization of material science and biology cells. Its principle is based on the series of projected image acquisitions at different inclination angles and its measurement of the volume of a tomogram (a three-dimensional, 3D, reconstruction) using a unique algorithm [9]. The utility of the combined STEM-in-SEM and ESEM had been explained by Bogner et al. [8], and this idea became a basic of the wet STEM imaging



mode development. The previous study has characterized particular materials in several transmission methods and has noticed beam widening through materials width. The result has shown that resolution, directly related to probe size, is subject to a top-down effect [10]. The use of thin materials/ samples thus results in a better resolution, avoiding the probe extending through the thickness of the sample/ material.

In the previous study, the minimum water layer determination was analyzed on the MCM-41 sample using wet-STEM [11]. The results explain STEM configuration on ESEM as a new approach to characterizing the three-dimensional structure of materials and optimizing the settlement of both resolution levels in several tens of nanometers and large tomogram sizes due to the high transparency thickness. Furthermore, by controlling the water pressure of the sample environment and controlling the sample temperature, STEM permits the observation of 2D transmission wet samples in ESEM [11].

The carbon material is easy to get since it is a vastly abundant material. This material has a symbol C with atomic number 6 and has four electrons to construct covalent chemical bonds. Carbon has a density of 2.267 g/cm^3 in graphite.

In this research, we perform the advisability of wet-Carbon compounds tomography by simulating the interaction of electron materials tomography in ESEM, which permits the acquisition of image sequences on wet materials. The sample used is carbon compounds which are widely used in industry. Then, the simulation of Monte Carlo will be used to estimate the optimum water thickness that can be detected on the wet sample.

Theoretical Background

We need to notice the STEM tomography technique's prominent parameters **in the Monte Carlo simulation**.

Tomography-STEM Technique

The tomography-STEM electron tomography technique is composed of three significant parts, specifically: (a) a system of *tilting*, (b) a system to keep the target area within the field of view, and (c) a system of detection [13]. The functions of each part are: (a) the system of *tilting* is a powerful microscope that permits the introduction of piezoelectric systems for more than 360° rotation around the horizontal axis; rotation was done accurately. (b) Systems to keep the desired areas within the field of view - a translational piezoelectric system- put the area of interest in the eccentric position before the image series acquisition. Then, suitable positioning of this area throughout addition is assured by the motion of the typical microscope phase. (c) A System of Detection: A ring-shaped detector is devoted to backscattering for wet STEM imaging trim. The collection of electrons is removed from its position and then placed under a thin sample; the electrons are transmitted indirectly (scattered) through the sample. The whole device is controlled and customized by the LabView software interface.

Each series of micrographs was obtained in the mode of STEM-in-SEM in circular darkfield conditions while the detector was placed under the rotating sample. The 3D structure was reconstructed using traditional software, including TomoJ [13].

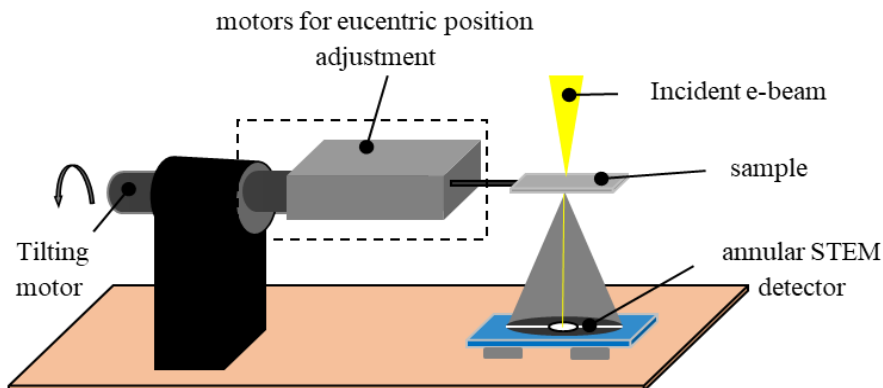


Figure 1. Schematic of the tomo-STEM tool [13]

Materials and Methods

We used a Hurricane software simulation that can be installed freely on a PC or similar device with a standard specification. Carlo decided that this product was free for the public and downloaded it on the official website, so he no longer uses USB hardware.

Simulation Methods, Conditions, and Parameters

The method we used was the electron scattering collection by using *Hurricane software* from SAMx (<http://www.samx.com/index.html.fr>) with the simulation of Monte Carlo. The previous research had also been conducted using the same tool (in both simulation and software) in the detection of MCM-41 material [9,11]. The preliminary phase of the simulation is determining the sample, which can be a pure compound material or a mixture. The material used is carbon, with and without a layer of water, which would be seen through the computation. In addition, we entered the carbon material by using the Hurricane software's compound menu, which contains some information on the compound that would be utilized in the simulation. We employed a 30 keV accelerating voltage as specified in the experiment for the computation. The option to set the maximum number of passes achieved during the simulation is one of the simulation parameters. For the simulation, we chose 100,000 passes because the bigger the value of passes, the slower the computation will be. The computation sample structure fits the criteria: $x = 5 \times 10^3$ nm, $y = 5 \times 10^3$ nm, and z-axis thickness variations range from 2×10^2 nm to 4×10^3 nm.

The mode of the batch simulation model was created to permit several simulations to be run concurrently and consecutively, with or without variations in deposit width. This is especially handy when one of the simulation parameters needs to be changed during the simulation. This study's simulation employed a spherical liquid precipitate with 1000 nm radius and width variations of the liquid layer at 10 nm, 20 nm, 30 nm, 50 nm, and 100 nm. The contrast variation was adjusted to 5% to establish the best water film thickness. The stages of the flowchart in this research are as follows.

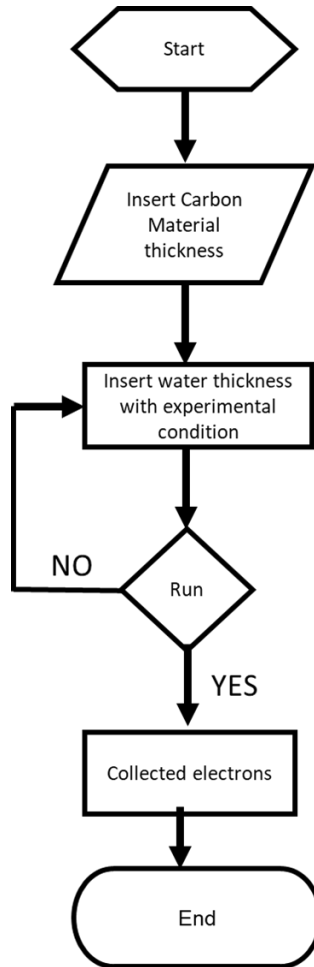


Figure 2. Flowchart Monte Carlo Simulation Stages

Results and Discussion

Determination of optimum water layer thickness with a variety of sample thicknesses carbon. Here we show the results of the Monte Carlo simulation on a computational box containing carbon thin films of varying thickness. They were coated with water with variations in thickness as well.

Electrons collected in the Monte Carlo simulation with water layer thickness variations in the carbon sample can be seen in Figure 3. The number of electrons used is 100,000, and the average number of electrons collected at a predetermined scattering angle is between 14° - 40° [9].

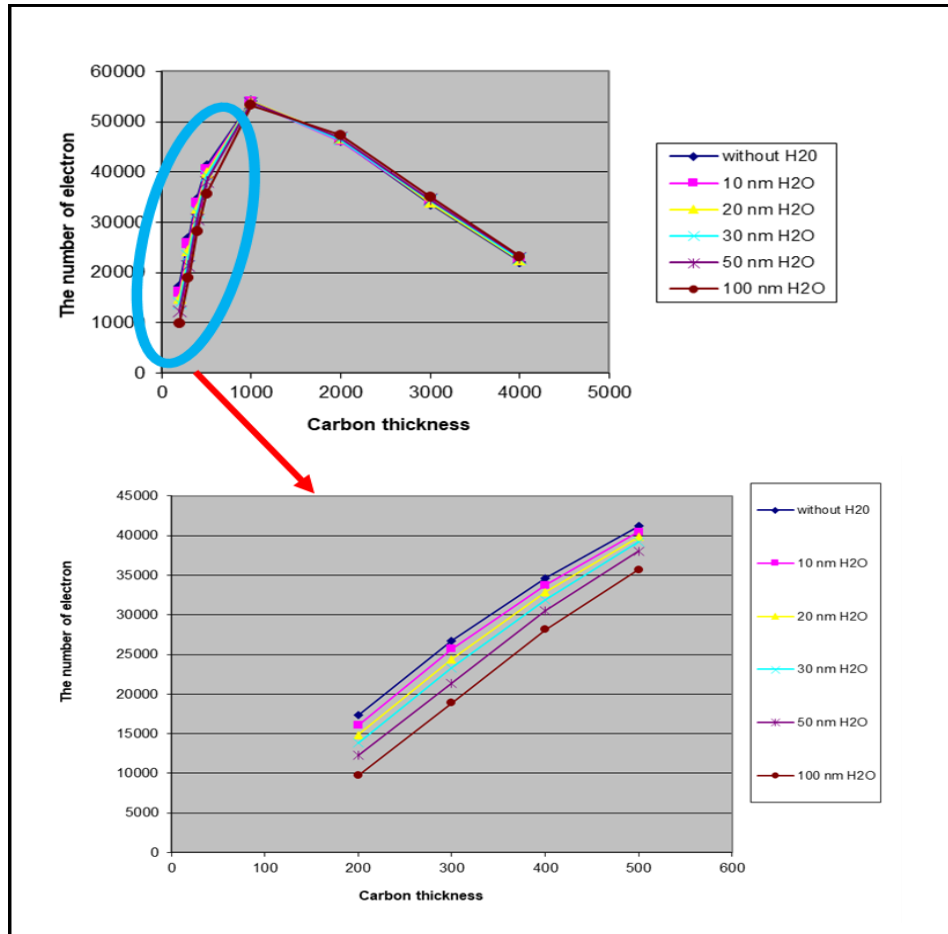


Figure 3. The average number of electrons collected at scattering angles between $14^\circ - 40^\circ$ on Carbon material with variations in the thickness of the water layer.

Figure 3 presents the optimum detectable water layer and shows that carbon with a thickness of 500 nm has a maximum point of the number of electrons collected. This represents that the greater the number of scattering electrons entering the dark circular field, the smaller the number of electrons collected at thicknesses above 500 nm. This can happen because the higher the thickness of carbon, the smaller electrons are captured since there are many electrons reflected out of the dark circular field. If we maximize the thickness of carbon from 0 to 500 nanometers, the difference for each thickness of water will be known respectively. All of the thicknesses carbon with water layers, the number of electrons relatively elevate between the thickness of water 200 nm and 500 nm. From here, we can determine the optimal thickness of the water.

Previous studies with different samples (MCM-41) stated that the curves for different thicknesses of water layers all had the same overall shape, with a maximum thickness of MCM-41 (equal to 2 m) [9]. For the thickness of MCM-41, which is thinner than 1 m, the number of electrons increases as the increase in sample thickness causes an increase in the number of scattering events and scattering angles. On the other hand, for MCM-41, which is thicker than 2 m, an increase in the number of scattering events still leads to an increase in scattering angle, exceeding the maximum gathering angle [9,11].

In the case of carbon, the number of electrons collected escalates until the thickness of 500 nm, and the scattering angle elevates as the electron scattering increases. For sample thicknesses above 500 nm, the collection angle will be more than 40° , so it will induce a decrease in electron collection.

The number of electrons leaving the sample is slightly affected by the layer of water above it. Nothing else affects the number of electrons collected by the detector. Therefore, the Monte Carlo simulation is likely to calculate the optimal water layer in which electrons can be detected at any material thickness.

Contrast Variation

Water condenses on the sample as the partial pressure of water rises, resulting in contrast fluctuations. Figure 4 depicts the projected difference in contrast between dry and wet circumstances. This information relates to the possibility of detecting a water coating on carbon. To get the preferable water width, we set the contrast variation to be larger than five percent ($\geq 5\%$) [9] [11].

Figure 4 shows how we can identify the best water layer to detect by taking the width of carbon with a contrast fluctuation greater than 5% or equal, and the results are shown in Figure 4. The optimal contrast variation has been set at 5%, and the rising thickness of carbon indicates the transition from dry to wet circumstances. For each thickness of carbon, a 5% variation, in contrast, is noted. The ideal water thickness was calculated using the contrast variation for each sample thickness.

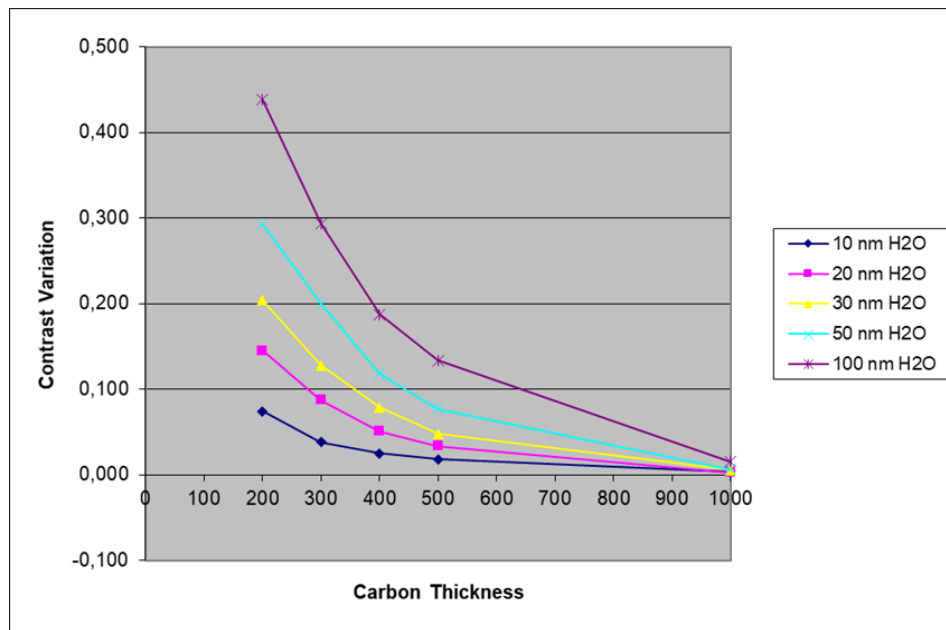


Figure 4. Expected dry to wet contrast variation conditions, in a function of carbon's matrix thickness

The Monte Carlo simulation calculates contrast variation, which explains how a specific area may be separated from the water layer. The formula is as follows:

$$\text{Contrast Variation} = \frac{N_{dry} - N_{wet}}{N_{dry}} \times 100\% \quad (1)$$

Where n_{dry} and n_{wet} correspond to the number of collected electrons in the desired area with no water layer and a pure water layer of the same thickness [14].

At a certain thickness of a material, the thicker the material, the greater the optimum thickness of the water obtained. The number of electron scattering caught is more significant so that the contrast of the image obtained is more evident.

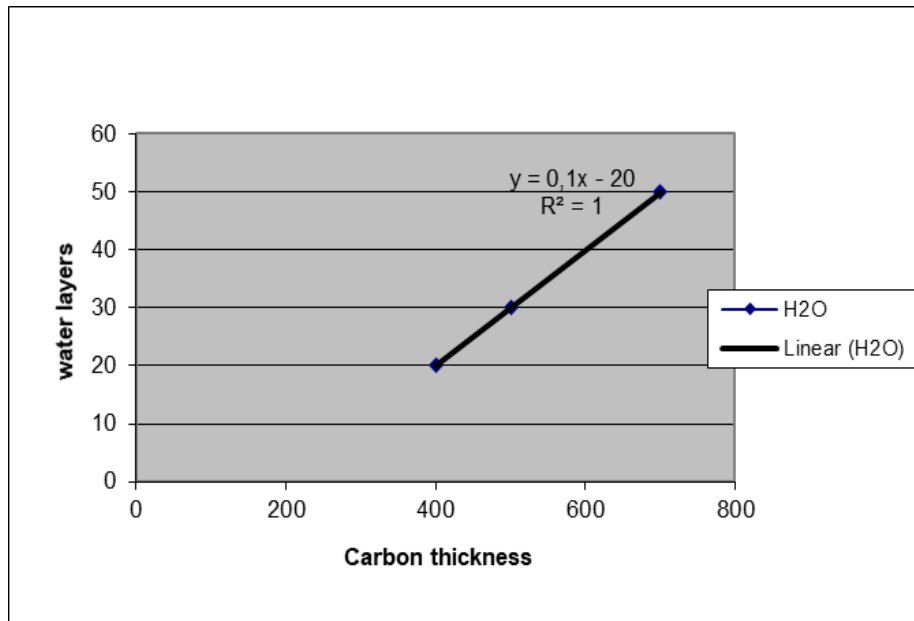


Figure 5. Contrast variation in carbon in the optimum water layer (electron collected)

On carbon with thicknesses of 400 nm, 500 nm, and 700 nm, the best water layer thicknesses that may be detected are 50 nm, 30 nm, and 20 nm, respectively. Surprisingly, the ideal water and carbon sample thickness have a linear relationship (Figure 5). Three of the five water resistance data are taken in Figure 5, and the three data taken are perfect linearity data. The link between the ideal value of water and the thickness of carbon is also shown in Figure 5, suggesting that the higher the thickness of carbon, the higher the optimum number of water required. This means that the more carbon and water between them, the more electrons water can collect.

Monte Carlo electron trajectory simulation of the interaction volume

We may calculate the dimensions of the volume interaction of simple material, such as carbon, using the Kanaya-Okayama formula stated in equation (1). Simultaneously, Monte Carlo simulations of "bulk materials" produce electron trajectories, with the interaction volume as the limiting factor (as shown in Figure 5 for the Carbon example). With a computational box sample structure, we have several material thickness parameters: $x = 33 \times 10^3$ nm, $y = 33 \times 10^3$ nm, and $z = 20 \times 10^3$ nm. The dimensions of the interaction volume are calculated using this parameter.

The dimension of volume interaction on carbon compounds determined from the simulation was found to be eight (8) microns, which is consistent with the Kanaya-Okayama formula (9 microns). This confirms how we derive the volume interaction boundaries from Monte Carlo findings. Still, it also allows us to specify the volume interaction dimensions of all materials under consideration. Moreover, the size of the volume interaction is a major function of the incident beam's energy as well as the chemical's structure and density. Kanaya Okayama's Formula is as follows:

$$R = (0.0276AE^{1.67}) / Z^{0.89} \quad (2)$$

Where

- R : the dimension of interaction volume
- A : relative atomic mass (g/mol)
- Z : atomic number
- ρ : density (g/cm²)
- E : energy of incident light (keV)

Figure 6 depicts the electron paths utilized in the Monte Carlo simulation to determine the volume interaction or the depth dimensions the electrons can travel. The electrons will be scattered, indicated by electron trails when the incident ray is shot; this Monte Carlo simulation demonstrates the existence of electron traces fired by incoming light with an energy of 30 kV.

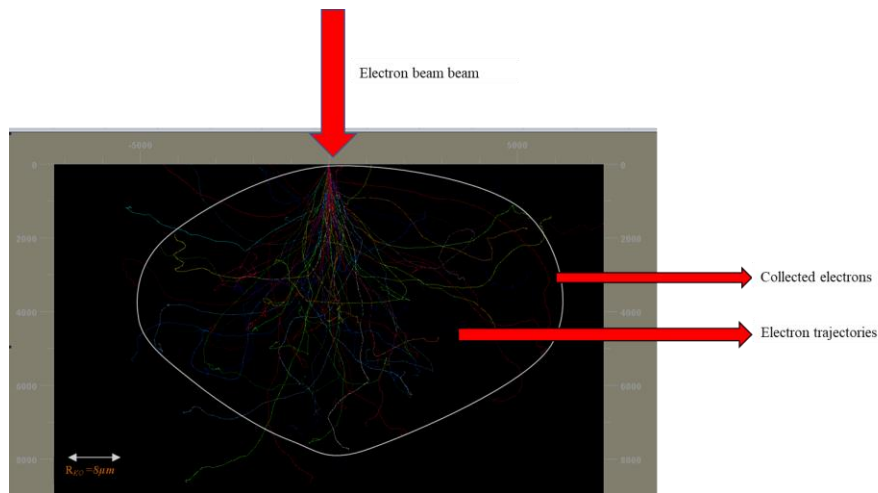


Figure 6. Monte Carlo electron trajectory simulation of the interaction volume in carbon as a function of the incident radiant energy of 30 keV with a sample thickness of 20,000 nm.

Conclusions

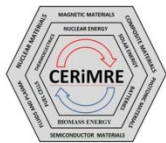
The experimental arrangement was simulated using simulations in STEM-in-SEM images. The pathways of 100,000 electrons were calculated using unique software, the Monte-Carlo approach (Hurricane program). This simulation allowed us to compute the optimum water layer thickness detected in carbon material. Although the relationship is thought to be linear between the ideal water film and sample thickness, the equation is



dependent on the sample's chemical structure and density. The empirical relationship between the optimum water layer thickness and the sample layer includes measuring the density and interaction volume. It will be fascinating to test the validity of the empirical findings in future work.

References

- [1] J. Xiao, G. Foray, and K. Masenelli-Varlot, 2018, *Analysis of liquid suspensions using scanning electron microscopy in transmission: estimation of the water film thickness using Monte-Carlo simulations*, J. Microsc., vol. 269, no. 2, pp. 151–160, doi: 10.1111/jmi.12619.
- [2] G. Foray, S. Cardinal, A. Malchere, and J. M. Pelletier, 2012, *Mechanical spectroscopy, a tool to characterize cement latex composites*, Solid State Phenom., vol. 184, pp. 399–404, doi: 10.4028/www.scientific.net/SSP.184.399.
- [3] P. Yu, B. Cui, and Q. Shi, 2008, *Preparation and characterization of BaTiO₃ powders and ceramics by sol-gel process using oleic acid as surfactant*, Mater. Sci. Eng. A, vol. 473, no. 1–2, pp. 34–41, doi: 10.1016/j.msea.2007.03.051.
- [4] G. Spina, G. Bonnefont, P. Palmero, G. Fantozzi, J. Chevalier, and L. Montanaro, 2012, *Transparent YAG obtained by spark plasma sintering of co-precipitated powder. Influence of dispersion route and sintering parameters on optical and microstructural characteristics*, J. Eur. Ceram. Soc., vol. 32, no. 11, pp. 2957–2964, doi: 10.1016/j.jeurceramsoc.2012.02.052.
- [5] H. Stahlberg and T. Walz, 2008, *Molecular electron microscopy: State of the art and current challenges*, ACS Chem. Biol., vol. 3, no. 5, pp. 268–281, doi: 10.1021/cb800037d.
- [6] A. M. Donald, 2003, *The use of environmental scanning electron microscopy for imaging wet and insulating materials*, Nat. Mater., vol. 2, no. 8, pp. 511–516, doi: 10.1038/nmat898.
- [7] D. J. Stokes, B. L. Thiel, and A. M. Donald, 1998, *Direct observation of water-oil emulsion systems in the liquid state by environmental scanning electron microscopy*, Langmuir, vol. 14, no. 16, pp. 4402–4408, doi: 10.1021/la980281c.
- [8] A. Bogner, G. Thollet, D. Basset, P. H. Jouneau, and C. Gauthier, 2005, *Wet STEM: A new development in environmental SEM for imaging nano-objects included in a liquid phase*, Ultramicroscopy, vol. 104, no. 3–4, pp. 290–301, doi: 10.1016/j.ultramic.2005.05.005.
- [9] K. Masenelli-Varlot et al., 2014, *Wet-STEM tomography: Principles, potentialities and limitations*, Microsc. Microanal., vol. 20, no. 2, pp. 366–375, doi: 10.1017/S1431927614000105.
- [10] L. Reimer, 1974, *Transmission Electron Microscopy of Thick Amorphous*, vol. 100, no. June 1973, pp. 81–92.
- [11] R. F. Septiyanto, K. Masenelli-Varlot, and F. Iskandar, 2014, *Simulation of electron-matter interaction during wet-STEM electron tomography*, AIP Conf. Proc., vol. 1586, no. November 2015, pp. 82–85, doi: 10.1063/1.4866735.



- [12] S. Banerjee, S. Dubey, R. K. Gautam, M. C. Chattopadhyaya, and Y. C. Sharma, 2019, *Adsorption characteristics of alumina nanoparticles for the removal of hazardous dye, Orange G from aqueous solutions*, Arab. J. Chem., vol. 12, no. 8, pp. 5339–5354, doi: 10.1016/j.arabjc.2016.12.016.
- [13] P. Jornsano, G. Thollet, J. Ferreira, K. Masenelli-Varlot, C. Gauthier, and A. Bogner, 2011, *Electron tomography combining ESEM and STEM: A new 3D imaging technique*, Ultramicroscopy, vol. 111, no. 8, pp. 1247–1254, doi: 10.1016/j.ultramic.2011.01.041.
- [14] J. Xiao, L. Roiban, G. Foray, and K. Masenelli-Varlot, 2018, *Characterization of Liquid Suspensions in 3D using Environmental Scanning Electron Microscopy in Transmission*, Microsc. Microanal., vol. 24, no. S1, pp. 350–351, doi: 10.1017/s1431927618002246.